G.J. van Rooij, J.W. Coenen, L. Aho-Mantila, M. Beurskens, S. Brezinsek,
M. Clever, R. Dux, C. Giroud, M. Groth, K. Krieger, S. Marsen, G.F. Matthews,
G. Maddison, A. Meigs, R. Neu, T. Pütterich, A.C.C. Sips, M.F. Stamp,
W.A.J. Vijvers, P. de Vries and JET EFDA contributors

Characterization of Tungsten Sputtering in the JET Divertor

Characterization of Tungsten Sputtering in the JET Divertor

G.J. van Rooij[1], J.W. Coenen[2], L. Aho-Mantila[3], M. Beurskens[4], S. Brezinsek[2], M. Clever[2], R. Dux[5], C. Giroud[4], M. Groth[6], K. Krieger[5], S. Marsen[5], G.F. Matthews[4], G. Maddison[4], A. Meigs[4], R. Neu[5], T. Pütterich[5], A.C.C. Sips[7], M.F. Stamp[4], W.A.J. Vijvers[8], P. de Vries[1] and JET EFDA contributors*

JET-EFDA, Culham Science Centre, OX14 3DB, Abingdon, UK

[1]*Dutch Institute For Fundamental Energy Research, Assoc. EURATOM-FOM, The Netherlands[†]*
[2]*Institute of Energy and Climate Research, Forschungszentrum Jülich, Assoc. EURATOM-FZJ, Germany[†]*
[3]*VTT, P.O. Box 1000, FI-02044 VTT, Finland*
[4]*EURATOM-CCFE Fusion Association, Culham Science Centre, OX14 3DB, Abingdon, OXON, UK*
[5]*Max-Planck-Institut für Plasmaphysik, EURATOM Association, Garching, Germany*
[6]*Aalto University, Association EURATOM-Tekes, Espoo, Finland*
[7]*European Commission, Brussels, Belgium*
[8]*Ecole Polytechnique Fédérale de Lausanne (EPFL), Centre de Recherches en Physique des Plasmas (CRPP), Association EURATOM – Confédération Suisse, CH*
[†]*Partner in the Trilateral Euregio Cluster*
* See annex of F. Romanelli et al, "Overview of JET Results",
(24th IAEA Fusion Energy Conference, San Diego, USA (2012)).

ABSTRACT

Tungsten erosion in the outer divertor of the JET ITER like wall was quantified by spectroscopy. Effective sputtering yields of $\sim 10^{-4}$ were measured in L-mode at ~ 30eV low recycling divertor conditions and Be was identified as the main species causing the sputtering. The signature of prompt redeposition was observed in the analysis of WI 400.9nm and WII 364nm line ratios indicating >50% redeposition fraction. Inter- and intra-ELM sputtering were compared for an example of 10Hz ELMs with 13MW NBI heating, in which intra-ELM sputtering was found to dominate by a factor of 9. Nitrogen seeding initially increased the tungsten sputtering threefold due to higher extrinsic impurity levels and effectively reduced the tungsten sputtering when the divertor plasma temperature was decreased from 25eV to 15eV.

1. INTRODUCTION

The current design of ITER projects tungsten (W) as plasma-facing components (PFCs) in the divertor for its active phase. Physical sputtering of W by impurities, in particular when extrinsic impurities are seeded, may compromise the life time of the PFCs as well as cause deterioration of the fusion performance by radiation due to unduly high W concentrations in the centre. In this contribution, we utilize the present ITER-like Wall (ILW) at JET to gain insight into ITER-relevant aspects of W erosion such as impurity flux density, charge state and impact energy [1].

A systematic spectroscopic study of L-mode and H-mode discharges with auxiliary heating by RF or NBI was performed using various W (W I) and $^+$ (W II) spectral lines to quantify the W source strength at the solid W outer divertor target subject to the local plasma conditions. A consistency analysis is performed by comparing the various spectral lines as well as by placing the source strengths in the context of the spectroscopically determined impurity species distribution and simple erosion estimates using Bohdansky's formula for low-energy ion sputtering. Experiments in H-mode are used to distinguish between inter- and intra-ELM sputtering profiles. Finally, impurity seeding is employed to assess the trade-off between introducing more sputtering particles and lowering the impact energy thereof by plasma cooling.

2. EXPERIMENTAL

Several spectroscopic systems were used to monitor the WI line radiation at 400.9nm at the horizontal target in the JET outer divertor. The primary diagnostic used in this study is a re-designed mirror-link system viewing the target from the top of the vessel and measuring the light in three wavelength ranges with Czerney-Turner spectrometers [2], to which we will refer as *spec-mirror*. The default settings of the system were 25Hz repetition rate, a spectral range of 395-409nm, and 20 lines of sight covering 360mm of the outer divertor. With a second system, the outer divertor area is viewed, again from the top of the vessel, by 10 lines of sight, each covering 20mm diameter spots at the divertor target. The light is relayed by fiber optics to Photo Multiplier Tubes equipped with 400.9nm bandpass filters (1nm bandwidth), providing a time response of up to 10kHz (referred to as *PMTs*)

or to one of four tunable Czerney-Turner spectrometers (referred to as *spec-fiber* [3]). A schematic view of the lines of sight of the three spectroscopic systems is shown in Fig.1

The measured line intensities were transformed into W particle flux densities using the number of ionizations per emitted photon [4], i.e. the (S/XB) value. We used the following fit to incorporate its dependence on the plasma temperature as was found by recent experiments at the TEXTOR tokamak in combination with experimental results from other devices [5]:

$$S/XB\ (T_e) = 53.7\ [1 - 1.04\ \exp(-\ T_e/22.1)] \tag{1}$$

Langmuir probe measurements were used to determine profiles of the divertor plasma temperature as well as the incident plasma flux densities.

3. RESULTS

3.1. W SPUTTERING IN L-MODE: ASSESSMENT OF THE SPUTTERING SPECIES

The W erosion in the JET outer divertor was evaluated as a function of the divertor electron temperature in L-mode discharges with 1 MW auxiliary heating by neutral beams. Data were obtained from three discharges. One was a scan of the divertor temperature from 43eV down to 17eV by means of varying the divertor fueling rate (JET Pulse No: 82195). Two discharges contained each three steps in the divertor density in which the divertor temperature was finally lowered to 7eV (JET Pulse No's: 81474 and 81486). The peak W particle flux densities were normalized to the saturation current measured by Langmuir probes at the same radial position. This number shall be referred to as the "effective" erosion yield, as is common practice, to express that the majority particle (deuterium) is not the sputtering particle. The results are plotted in Fig.2 as a function of the divertor plasma temperature derived from the same Langmuir probe. For comparison, the sputter yield is indicated for an admixture of 0.5% of Be^{2+} and C^{4+} (these charge states are in Coronal equilibrium most abundant for $20 < T_e < 35eV$).

The plot shows that the measured effective erosion yield increases monotonically in the temperature range $15 < T_e < 45eV$ but no threshold behavior is encountered in the data from the density ramp. However, the pulses with the density steps did achieve the W signal to drop to close to the detection limit. These points match the threshold behavior that corresponds to Be^{2+}.

It is seen that a fraction of 0.5% beryllium (Be) in the target flux density is sufficient to explain the observed W sputter signal. This number is in excellent agreement with the intensity of the BeII 527 nm line as it was measured with the PMTs. The signal integrated over the entire horizontal target was typically $(1.2 \pm 0.24) \times 10^{18}$ photons $m^{-2}s^{-1}$, which translates (with S/XB = 70) into 8.4×10^{19} Be atoms $m^{-2}s^{-1}$. This value corresponds for the actual variation in the target saturation current to a fraction of 0.35% up to 0.50%. It is noted that the fraction of Be in the target flux had apparently been lower than the Be fraction in the main plasma for these particular discharges. Assuming Be as the only impurity in the main plasma, we estimated its concentration from the effective charge

2

(Z_{eff}), which ranged from 1.2 to 1.4 for the discharges under evaluation: 1.8% - 3.6%. Preliminary charge exchange results confirmed such Be concentrations in the main plasma.

We thus conclude that sputtering by Be only explains the entire observed W sputter rate. Still, let's confirm here that sputtering by other impurities is not important. For the case under evaluation, we therefore assessed the contribution of carbon. PMT measurements are available for the CIII 465nm line and give a ~8 times larger integrated photon intensity for the horizontal target compared to the BeII 527nm line. Multiplied with the respective photon efficiencies of 1 and 70, this implies a factor of 10 lower carbon flux density compared to the Be flux density, i.e. a carbon fraction of ~0.05%, of the total particle flux. Assuming the helium-like charge state of 4+ for the carbon, such a fraction implies that the contribution of carbon to the W sputtering is roughly a factor of 5 lower than the sputtering by Be. The unimportance of carbon in the operation of the JET ILW was observed throughout the 2011/2012 JET campaigns as concentrations were generally in the 0.05% concentration range [6].

Qualitative information, but with more spatial and spectral resolution, was available from the *spec-fiber* system. Comparing intensity profiles learned that the spatial profile of the CIII 465nm line radiation was much wider than for the BeII 527nm line or e.g. the CII 515nm, the latter two being more alike. The intensity ratio CII/BeII was 0.6, i.e. a particle flux ratio C/Be of 0.08. These numbers confirm again that sputtering by carbon impurities is negligible compared to sputtering by Be.

3.2. W SPUTTERING IN LOW DENSITY L-MODE DISCHARGES WITH LARGE SAWTEETH INDUCED TEMPERATURE EXCURSIONS

The dependence of the W sputtering on both the Be flux and the divertor plasma conditions was investigated in a larger parameter range by analyzing discharges with 1-3MW ICRH auxiliary heating at medium to low line averaged plasma density (1.6-2.8×10^{19} m^{-3}). Characteristic of these discharges were the strong oscillations in the divertor plasma temperature (and target flux density). These temperature oscillations had amplitudes of up to 20eV and induced correlated oscillations in the fast PMT measurements of the WI photon fluxes. The time resolution of the measurements allowed to relate the instantaneous WI photon (or particle) fluxes and divertor conditions and evaluate again the effective erosion yields as a function of plasma temperature, i.e. energy of the sputtering particle. The results of the analysis are plotted in Fig.3. It is seen that the increase of the W sputtering with divertor temperature is similar as before, but it also depends on the total heating power and on the main plasma density. The effect of the heating power relates to an increasing Be content in the plasma and thus increasing Be influx in the divertor. Both the analysis of Z_{eff} of the main plasma and the BeII photon fluxes in the outer divertor indicate this and are in line with the general observation that RF power leads to additional Be sputtering [7]. However, the observed increases in Z_{eff} did not account for the observed increase in W sputtering at the lower densities and the reasons for this are presently not clear. Possible effects playing a role here include uncertainties

in the relation between the Langmuir probes temperature measurements and the impact energy of the sputtering particles, a plasma density dependence of the WI S/XB values, the appearance of other sputtering impurities or changes in the (non-coronal) charge state distributions.

3.3. W SPUTTERING IN H-MODE: INTER- VERSUS INTRA-ELM SPUTTERING

The large difference between inter- and intra-ELM W sputtering in H-mode is illustrated by the W influx profiles that are shown in Fig.4. The 40 ms time resolution of the *spec-mirror* system was insufficient to resolve ELMs and therefore, an example was chosen in which the ELM frequency was sufficiently low to record (by coincidence) spectra containing the contribution of one single ELM and spectra without any ELM contribution. The PMT measurements confirmed this method for the profiles presented.

For the specific example, the inter-ELM sputtering amounted to 6.3×10^{18} atoms/s (following from integration over the entire outer strike point and using S/XB = 30 on basis of the measured inter-ELM 17eV divertor temperature). The inter-ELM total saturation current in the outer divertor was 1.7×10^{23} el/s, which means that the effective inter-ELM sputter yield amounted 4×10^{-5} and was thus similar to the L-mode sputter yields that were determined above. The intra-ELM sputtering was 4.7×10^{18} atoms/ELM (subtracting the inter-ELM sputtering from the profiles containing the intra-ELM sputtering and using S/XB=50 on basis of a roughly estimated intra-ELM divertor temperature of 80eV). Given the 10 Hz ELM frequency, this means that intra-ELM sputtering dominated by a factor of 9 over inter-ELM sputtering and thus a discharge averaged effective erosion yield of 4×10^{-4}.

3.4. WII SPECTROSCOPY AND W PROMPT REDEPOSITION

A consequence of the grazing angle incidence of the magnetic field with the divertor target is that most of the sputtered particles will return to the surface when the ionization mean free path of the sputtered W atoms becomes smaller than the ion Larmor radius. [8,9]. The promptly redeposited fraction can experimentally be investigated by comparing spectral lines of neutral W and ionized W [10]. The rationale is that the S/XB for neutral W lines is unaffected by redeposition ''losses'', whereas these do form an addition loss channel for ionized particles. Thus, assuming a redeposition rate R, the photon efficiency *(S/XB)_{ion}* transforms into *((S+R)/XB)_{ion}*.

A spectrum recorded in discharge JET Pulse No: 80896 around 364nm, where suitable WII lines can be found, is shown in Fig.5. In addition to the W lines, also chromium and nickel lines are recognized (from Inconel support structures in the main vessel, probably transiently deposited at the strike point position). The two highlighted spectral lines were selected for the WII/WI line ratio analysis. The WI 361.7nm line was selected on basis of its high intensity as well as strong correlation with the WI 400.9nm line. The WII is obviously selected also for its intensity, but moreover as information on its S/XB values is available from modeling [11]. For the present analysis, we have not applied the calculated S/XB values because the uncertainty in the W ground state level population

introduces an uncertainty in the S/XB value of an order of magnitude. Instead, the line intensity ratios Φ_{WII}/Φ_{WI} were evaluated for the discharges JET Pulse No's: 80893 and 80896 around $t =$ 60s, which means for divertor electron densities of 0.4×10^{19} m^{-3} and 1.2×10^{19} m^{-3}, respectively (measured by Langmuir probes at the strike point). The line ratios were 2.1 ± 0.2 and 1.1 ± 0.3, respectively (the difference in relative accuracy is due to the much lower line intensities at the higher plasma density). In other words, indeed a significant change is observed in the line intensity ratio. The observed change in the line intensity ratio can be put in the context of a change in the promptly redeposited fraction by assuming that the two density cases differ only in the promptly redeposited fraction and in the W sputter rate. We find using the effective inverse photon efficiency *(S+R)/XB* for the two density cases *a*, i.e. 0.4×10^{19} m^{-3}), and *b*, i.e. 1.2×10^{19} m^{-3}:

$$(\Phi_{WII}/\Phi_{WI})_a/(\Phi_{WII}/\Phi_{WI})_b = (S + R_b)/(S + R_a) = 1.9. \qquad (2)$$

With this relation, a minimum value for the redeposited fraction at density *b* can be estimated by setting the redeposition rate $R_a = 0$. This yields $R_b = 0.9S$, i.e. approximately equal to S and thus (a minimum of) ~50% of the particles is promptly redeposited. We note the agreement of the value with results from local injection of WF$_6$ at the twin limiters in TEXTOR under similar n$_e$ and T$_e$ conditions, which also yielded a promptly redeposited fraction of 50% [10].

3.5. NITROGEN SEEDING

Impurity seeding has been successful for reducing power and energy loads on divertor targets (e.g. [12,13] and references therein). However, in the ILW environment it will significantly increase the W sputter rate if the added extrinsic impurity dominates over the decreased impact energy due to lower divertor plasma temperatures. This balance is illustrated by a series of pulses (JET Pulse No's: 82293-82296: 1.1MW NBI heating) in which nitrogen (N) was seeded at different rates (4×10^{21} – 1×10^{22} el/s) in the divertor. The N flux to the target was monitored via the NIII 403.5nm line. This flux is observed to build up during the discharge although the seeding level is being kept constant, a feature that is generally known for N seeding. The left panel in Fig.6 shows that the divertor N temperature is determined by the N flux and that it decreases from initially 25eV at the lowest seeding rate down to finally 5 eV at the highest seeding rate. The right panel shows the W particle flux as determined from the WI line intensity versus the divertor plasma temperature (controlled by the N flux). The plot confirms the expected trend. Starting from the highest temperatures, the W sputtering increases steeply (due to sputtering by N). A maximum sputtering is observed around 20eV, i.e. here the effect of plasma cooling starts to dominate. The nitrogen seeding has a net beneficial effect on the W erosion when the temperature is dropped below 15eV.

CONCLUSIONS

The W source in the outer divertor of JET in its ITER-like wall configuration, which is the region

in which W sputtering is maximum, has been quantified under various experimental conditions from spectroscopic observation of the horizontal target plate that consists of solid W lamellae. We conclude that the erosion is mainly caused by Be, which is also the dominant impurity in the plasma. An estimate from spectroscopic signals indicates that the carbon fraction in the target flux is only 0.05%. We have established experimental evidence that sputtering during ELMs dominates over in-between ELM sputtering, for the presented example by a factor of 9. The promptly redeposited fraction was assessed by comparing neutral W and W ion lines and yielded a lower limit of 50%. Finally, the balancing in N-seeding between additional sputtering due to the presence of N and reduced sputtering due to divertor cooling was illustrated.

ACKNOWLEDGEMENT

REFERENCES

[1]. G.J. van Rooij et al., 20th International Conference on Plasma Surface Interaction in Fusion, Aachen, Germany, 2012.

[2]. A. Meigs et al., Review of Scientific Instruments **81** (2010) 10E532.

[3]. M.F. Stamp et al., Journal of Nuclear Materials **337–339** (2005) 1038.

[4]. K. Behringer et al., Plasma Physics and Controlled Fusion **31** (1989) 2059.

[5]. M. Laengner et al., 20th International Conference on Plasma Surface Interaction in Fusion, Aachen, Germany, 2012.

[6]. S. Brezinsek et al., 20th International Conference on Plasma Surface Interaction in Fusion, Aachen, Germany, 2012.

[7]. C. Kleppers et al., 20th International Conference on Plasma Surface Interaction in Fusion, Aachen, Germany, 2012.

[8]. D. Naujoks. et al., "Tungsten as Target Material in Fusion Devices", Nuclear Fusion **36** (1996) 671.

[9]. G. Fussmann et al., Plasma Physics and Controlled Nuclear Fusion Research, 1995 (Proc. 15th Int. Conf. (Seville 1995)) vol 2 (Vienna: IAEA).

[10]. S. Brezinsek et al., Physica Scripta **T145** (2011) 014016.

[11]. A. Pospieszczyk et al., Journal of Physics B: Atomic, Molecular and Optical Physics **43** (2010) 144017.

[12]. J. Rapp et al., Nuclear Fusion **44** (2004) 312.

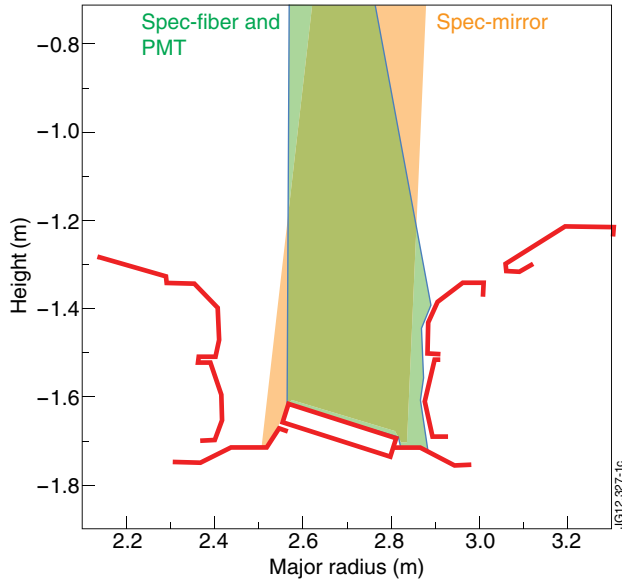[13]. C. Giroud et al., Nuclear Fusion **52** (2012) 063022.

Figure 1: Cross section of JET in which the lines of sight of the various spectroscopy systems are indicated. The "spec-mirror" system covers a chord of 360 mm long and therewith the horizontal target plate by 20 lines of sights in a mirror linked system. The "spec-fiber" and "PMT" systems view 10 chords of 20 mm diameter using fiber optics, therewith also covering the horizontal target plate.
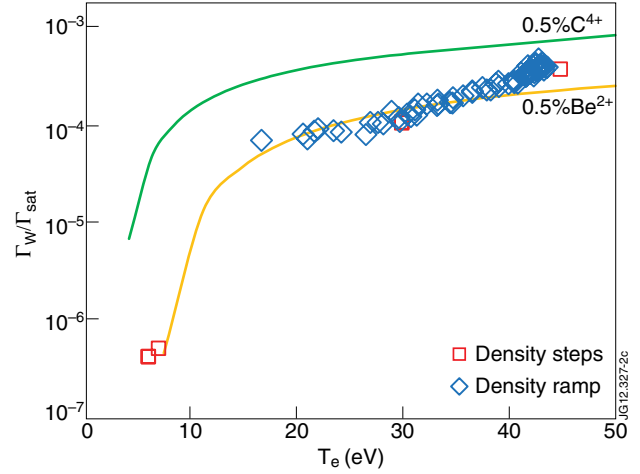

Figure 2: Effective erosion yields measured in L-mode with 1 MW NBI heating. The yields are compared with the calculated erosion yield for 0.5% Be^{2+} and 0.5% C^{4+} content in the particle flux.
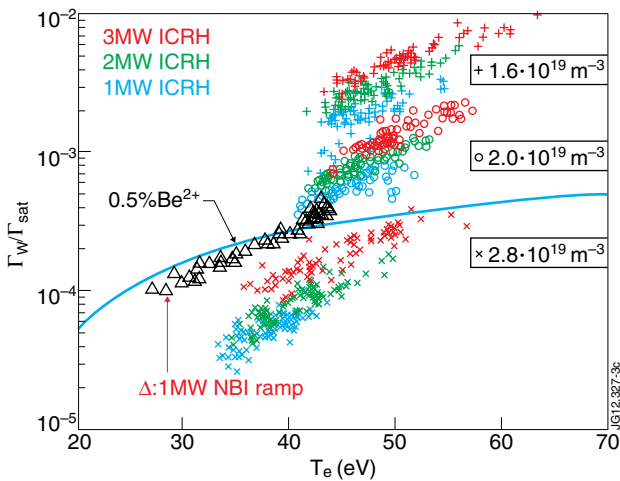

Figure 3: Effective erosion yields determined from the sawteeth dominated ICRH discharges (JET Pulse No's: 80889, 80893, 80896). The symbols refer to different main plasma densities, the colors refer to the different additional heating levels. For comparison, also the data from Fig.2 are included (black symbols).
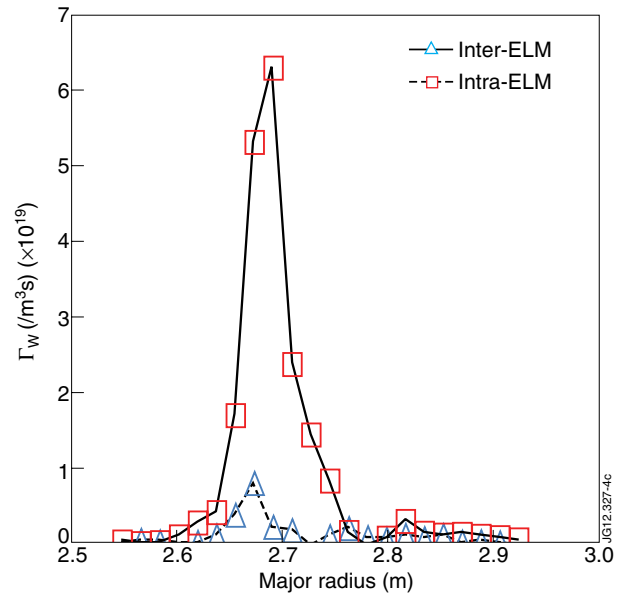

Figure 4: Comparison of the time averaged intra-ELM and the inter-ELM tungsten sputtering shows that intra-ELM sputtering is dominant. The outer divertor tungsten influx profiles were measured in discharge JET Pulse No's: 82237 (13MW NBI, 7.5×10^{19} m^{-3} line averaged n_e, 10Hz ELMs).
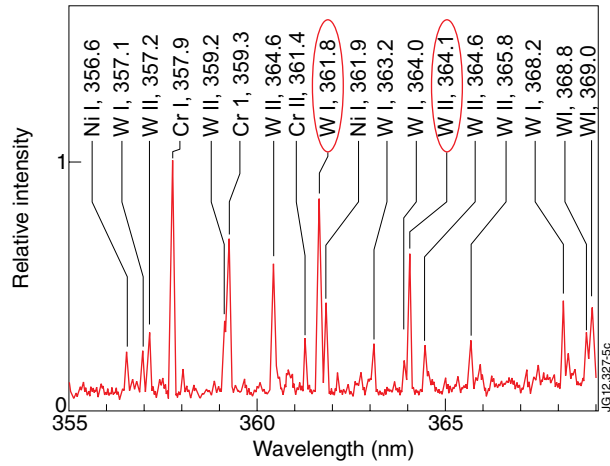
Figure 5: Identification WI and WII lines in a UV spectrum recorded in discharge JET Pulse No: 80896.
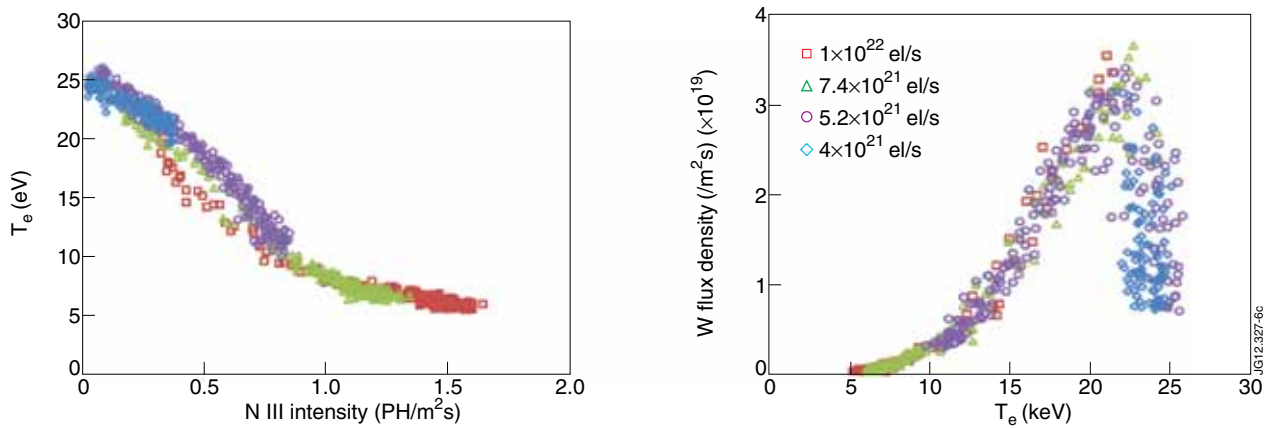

Figure 6: Effect of N seeding in the divertor. The left panel shows how the divertor plasma temperature drops as the N fluxes build up. The right panel shows that this initially increase in the W sputtering steeply due to higher impurity (N) target fluxes and subsequently plasma cooling takes over to decrease the sputtering.